

SPECKLE REDUCTION OF SYNTHETIC APERTURE SONAR IMAGES

S. A. Fortune*, M. P. Hayes and P. T. Gough

Acoustics Research Group, University of Canterbury, New Zealand

*Email: s.fortune@elec.canterbury.ac.nz

Abstract

Multi-look processing is a well known technique for reducing speckle in coherent imagery. This paper investigates the use of multi-look processing in range (frequency-compounding) on SAS images.

The coherence between sub-images produced by frequency compounding is determined and a coherence model proposed. This is used to calculate the level of speckle reduction for a given number of looks and spectral displacement. This shows that the optimal level of speckle reduction for a given loss in resolution is achieved when the spectral windows are displaced by approximately one third their bandwidth. The level of speckle reduction obtained using frequency compounding was measured for field SAS images and compared to the model. The number of looks used can be varied to trade-off the desired levels of speckle reduction and resolution loss. The number of looks that maximises the detectability ratio of speckle reduction to resolution loss is then experimentally measured.

Introduction

A synthetic aperture sonar (SAS) system coherently combines the collected data to increase the along-track resolution of the image. Due to the coherent nature of the imaging, speckle forms in the images. Speckle is a multiplicative noise which gives a variance to the intensity of each pixel. This reduces radiometric resolution. It also reduces spatial resolution. [1]. Speckle can also have a detrimental affect on some image processing techniques such as segmentation, classification, and autofocus using contrast optimisation [2].

Multi-look processing, or spatial and frequency compounding, is a well known and effective technique for reducing speckle noise and is used in ultrasound and synthetic aperture radar (SAR) imaging. It does however require a tradeoff between spatial and radiometric resolution. We wish to determine how to get the best reduction in speckle noise for a given loss in spatial resolution.

Other speckle reduction techniques can also be used, such as image-domain filters [4], adaptive filtering and wavelet-domain filtering. They are outside the scope of this paper.

In this paper we experimentally determine the coherence between the sub-images obtained when frequency compounding a SAS image and fit a model to it. This

is used to determine the theoretical limit to the amount the speckle can be reduced. The optimal displacement of the spectrum of each sub-image is thus determined. Using this displacement, the number of looks that maximises the detectability ratio of speckle reduction to resolution loss is shown.

The University of Canterbury has developed a sea-going towed SAS; KiwiSAS. The techniques outlined are applied to data collected from this platform.

Speckle Statistics

When a rough surface is illuminated by a coherent source, the measured field has a granular appearance with random intensity and phase known as speckle. The phase of a given pixel is uniformly distributed and the intensity is negative exponentially distributed with standard deviation equal to the mean when fully developed [3].

Over a whole image however, the mean intensity varies with range and with the presence of targets or other inhomogeneities. Thus the distribution of all pixels cannot be used to estimate the distribution of a single pixel. However, a small patch around a pixel, with constant mean intensity, can be used to estimate the distribution of a pixel within that patch.

Consider the complex-value image U with intensity $I = |U|^2$. Speckle contrast is defined as the ratio of the standard deviation of speckle intensity to the mean intensity.

$$C_s \equiv [\langle I^2 \rangle - \langle I \rangle^2]^{1/2} / \langle I \rangle. \quad (1)$$

For fully developed speckle images, $C_s = 1$. As the speckle noise is reduced, so does the speckle contrast. The signal to noise ratio of a speckle image is defined as the ratio of the mean image intensity and standard deviation, i.e.,

$$\text{SNR} = \langle I \rangle / [\langle I^2 \rangle - \langle I \rangle^2]^{1/2} = 1/C_s. \quad (2)$$

When evaluating the speckle contrast or SNR of an image, the contrast is evaluated for several small patches over the image, so that the mean intensity of a patch is roughly constant. The median value of all patches is used, to remove outliers such as those containing targets. This works well for bland images with localised structure as is typical for SAS images.

Multi-look Processing

Multi-look processing, also known as frequency or spatial compounding, splits the available data into a number of lower resolution 'looks' or sub-images of the object, then incoherently combines them back together to form an image with improved speckle characteristics and reduced spatial resolution. This relies on the fact that the speckle pattern has frequency and spatial dependence while any target does not.

In ultrasound and SAR, compounding is generally performed in the along-track direction. In SAR this is because the high Q nature of the imaging means it is easier to achieve high along-track resolution than high range resolution. However in SAS, due to the lower propagation speed of sound, it is easier to achieve high range resolution than high along-track resolution. For example, Kiwi-SAS obtains 4 cm range resolution and 16 cm along-track resolution. Thus we have chosen to perform frequency-compounding, or multi-look processing in the range direction.

To perform frequency-compounding, the image is Fourier transformed in the range direction and multiplied by N separate but overlapping windows of bandwidth W_i , each separated by a distance of δW_i . Each is then inverse Fourier transformed, giving N sub-images U_i . These parameters are related by

$$W_i = \frac{W}{1 + \delta(N - 1)}, \quad (3)$$

where W is the total spectral length of the image. This results in a resolution loss defined as $r \equiv W_i/W$.

To combine the sub-images, we sum intensities then take the square root i.e.,

$$\hat{U} = \left[\sum_{i=1}^N |U_i|^2 \right]^{1/2}. \quad (4)$$

This gives a slight reduction in noise standard deviation over summing amplitudes [6].

We are only considering the case of each sub-image having the same bandwidth and separation. Moreira [5] presents a technique using two different window sizes that claims to have increased speckle reduction for the same loss in resolution, but this will not be considered here.

When using overlapped windows, each sub-image has some coherence, so the speckle noise does not drop as much as if the looks were completely independent. A useful measure to compare the effectiveness of speckle reduction techniques is the effective number of statistically independent images N_{eff} that are contributing to the compounded image:

$$N_{\text{eff}} \equiv \left[\text{SNR}_N / \text{SNR}_1 \right]^2 = \left[1 / C_s(N) \right]^2. \quad (5)$$

Coherence of Sub-images

Consider the same object imaged with two different looks, U_i, U_j with $I_i = |U_i|^2$. We define the normalised coherence function between these two images as

$$\gamma_{ij} \equiv \frac{\langle U_i U_j^* \rangle}{[\langle I_i \rangle \langle I_j \rangle]^{1/2}} \quad (6)$$

If the N compounded sub-images are uncorrelated ($\gamma_{ij} = 0$ for $i \neq j$), compounding would result in a drop of speckle contrast of $1/\sqrt{N}$. If the sub-images are correlated the contrast drops as follows [8],

$$\begin{aligned} C_s(N) &= \frac{1}{N} \left[\sum_{i,j=1}^N |\gamma_{ij}|^2 \right]^{1/2} \\ &= \frac{1}{\sqrt{N}} \left[1 + 2/N \sum_{i=1}^{N-1} \sum_{j=i+1}^N |\gamma_{ij}|^2 \right]^{1/2} \end{aligned} \quad (7)$$

If the displacements between each image are constant, then the normalised coherence γ_{ij} is a Toeplitz matrix [8] with elements

$$\gamma_{ij} = \gamma(|i - j| \delta W_i). \quad (8)$$

Now (7) reduces to,

$$C_s(N, \delta) = \frac{1}{\sqrt{N}} \left[1 + \frac{2}{N} \sum_{m=1}^{N-1} (N - m) \gamma^2(m\delta) \right]^{1/2}. \quad (9)$$

Determining the Coherence Curve

Fig. 1 shows the measured image coherence of a field SAS speckle image. The fractional spectral separation δ between sub-images was increased and the sub-image bandwidth W_i held constant. Image coherence given by (6) was measured between all $(N - 1)$ adjacent sub-images and averaged.

We use a Gaussian to model the coherence curve, i.e.

$$\gamma(\delta) \approx \exp [-(\delta/\alpha)^2]. \quad (10)$$

A Gaussian model of sub-image coherence has successfully been used for ultrasonic images [9]. Justification for this is given by Wagner et al. [10], who proposed that the coherence function could be evaluated as the autoconvolution of the Fourier transform of the square of the beampattern. In our case, the beampattern is a sinc function, the Fourier transform of a sinc² is a triangular function and the convolution of two triangular functions gives a Gaussian approximation. The coherence curve in Fig. 1 is compared against the Gaussian model with $\alpha = 0.32$ showing a good match. To compare, Lorenz et al. [9] determined a value of

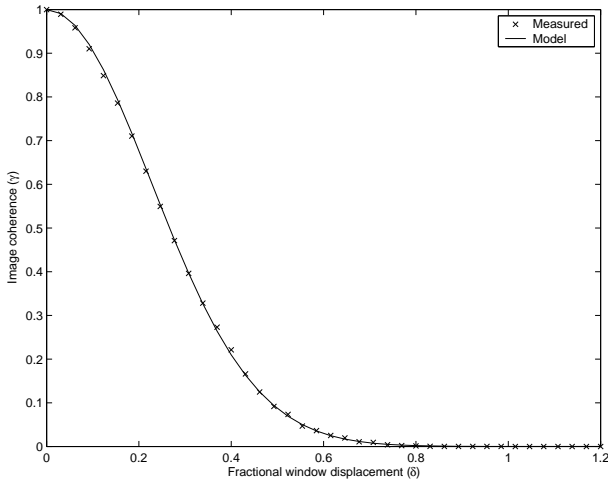


Figure 1: Image coherence of sub-images of field SAS speckle image, as a function of the fractional spectral displacement δ . The model is given by (10) with $\alpha = 0.32$.

$\alpha = 0.707$ for frequency compounding of ultrasonic images and O'Donnell et al. [11] determined a model for along-track spatial compounding of SAR images with an equivalent of $\alpha \approx 0.42$.

Results

The coherence model in (10) can be substituted into (9) to determine the theoretical speckle contrast of the compounded image. The resulting value of N_{eff} is shown in Fig. 2 as a function of δ , the fractional spectral displacement. This shows that an optimal reduction of speckle occurs when the spectral bands of the sub-images are displaced by approximately one third of their bandwidth. The location of this peak does not depend on the value of W_i used. It also shows a significant improvement in speckle reduction when using overlapping spectral bands ($N_{\text{eff}} = 3.4$) against using non-overlapping bands ($N_{\text{eff}} = 2$) for the same loss in resolution.

To compare, the optimal fractional displacement of the aperture for spatial compounding of ultrasound images is 0.5 [11]. Due to the higher measured correlation in their imaging, this corresponded to the equivalent of a maximum value of approximately $N_{\text{eff}} = 2.8$.

It is possible to trade off the desired level of speckle reduction N_{eff} and resolution loss r . Fig. 3 shows the theoretical value of N_{eff} from the model is approximately linear with r .

Field Data

Fig. 3 compares the measured amount of speckle reduction in a field SAS speckle image to that predicted by (9) using the Gaussian coherence model and $\alpha = 0.32$. The measured N_{eff} value is the median value of

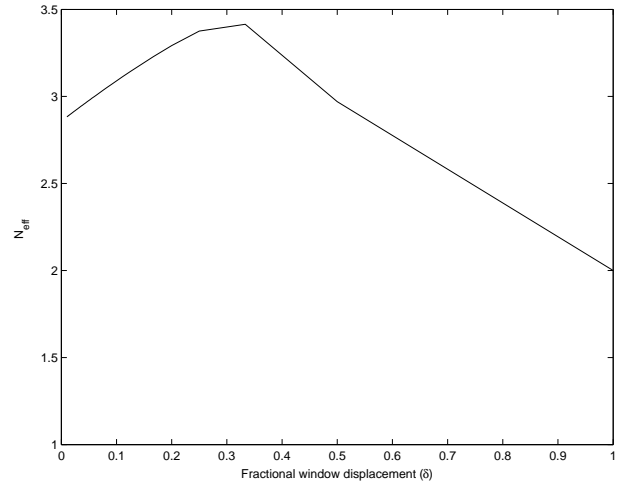


Figure 2: Predicted performance of range-compounding using coherence model in (10). Sub-image bandwidth (W_i) is kept constant at $W/2$.

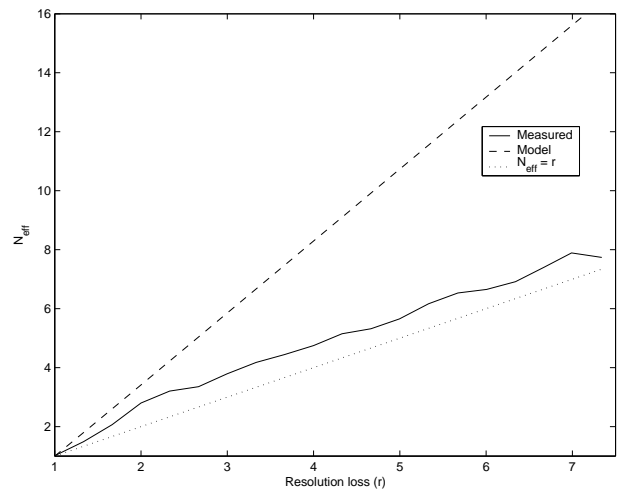


Figure 3: Range-compounding performance for $\delta = 1/3$. Measured data is from field SAS speckle image, model is predicted from coherence model (10).

the ratio of mean squared intensity to variance of intensity of various patches in the image. It shows the measured amount of speckle reduction is approximately half the optimal value predicted by the model. This is similar to results in ultrasound [9].

Detectability

In ultrasound, studies have shown that to optimise the detectability of lesions, you should maximise the ratio of speckle reduction to resolution loss N_{eff}/r [12]. However, it has been shown in ultrasound that speckle reduction does not increase this figure of merit [9]. Fig. 3 shows $N_{\text{eff}} > r$, therefore speckle reduction does increase this detectability figure in SAS. Fig. 4 shows the optimum number of looks for detectability is $N = 4$.

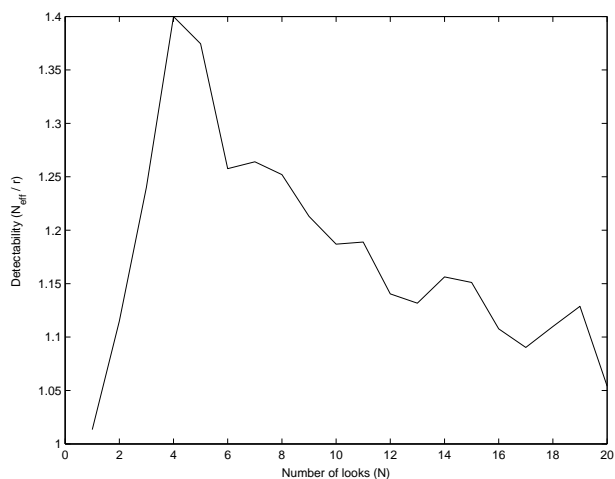


Figure 4: Detectability ratio N_{eff}/r versus number of looks for field SAS speckle image.

Conclusions

We have investigated the use of frequency compounding on SAS images. The coherence curve between sub-images was determined and a Gaussian was found to be an accurate model. Using this model, the level of speckle reduction for a given number of looks and given spectral displacement can be determined. This shows that using many overlapping windows gives a larger reduction in speckle for the same resolution loss. (Up to 1.7 times larger.) The reduction in speckle contrast, calculated using the coherence model, was found to be optimal for a displacement of the spectral windows by approximately one third of their bandwidth. Using this displacement, the number of looks can be varied trading off the amount of speckle reduction and resolution loss.

Range compounding was performed on field SAS data. The measured reduction in speckle was approximately half that predicted by the measured coherence model. The reasons for this could include less than full coverage of the spectral band and structure in the image increasing sub-image coherence.

The detectability ratio of speckle reduction to resolution loss can be improved by frequency compounding and is optimum for $N=4$ for our system. This gave a resolution loss of 2 and a measured $N_{\text{eff}} = 2.8$.

References

- [1] A. Kozma and C. Christensen, "Effects of speckle on resolution," *Journal of the Optical Society of America*, vol. 66, pp. 1257–1260, November 1976.
- [2] S. A. Fortune, M. P. Hayes, and P. T. Gough, "Contrast optimisation of coherent images," in *Oceans 2003, Marine Technology and Ocean Science Conference*, 2003.
- [3] J. W. Goodman, "Statistical properties of laser speckle patterns," in *Laser speckle and related phenomena* (J. C. Dainty, ed.), 1975, pp. 9–75, Springer-Verlag, Berlin.
- [4] F. K. Li, C. Croft, and D. N. Held, "Comparison of several techniques to obtain multiple-look SAR imagery," *IEEE Transactions on Geoscience and Remote Sensing*, vol. 21, pp. 370–375, July 1983.
- [5] A. Moreira, "Improved multilook techniques applied to SAR and SCANSAR imagery," *IEEE Transactions on Geoscience and Remote Sensing*, vol. 29, pp. 529–534, July 1991.
- [6] J. S. Lee, "Speckle suppression and analysis for synthetic aperture radar images," *Optical Engineering*, vol. 25, pp. 636–643, May 1986.
- [7] Y. Li, V. Newhouse, P. Shankar, and P. Karpur, "Speckle reduction in ultrasonic synthetic aperture images," *Ultrasonics*, vol. 30, no. 4, pp. 233–237, 1992.
- [8] S. D. Silverstein, "Coherence and speckle reduction in compounded correlated phased arrays: Synthetic aperture radar," *Journal of the Optical Society of America A*, vol. 3, pp. 1925–1934, November 1986.
- [9] A. Lorenz, L. Weng, and H. Ermert, "A gaussian model approach for the prediction of speckle reduction with spatial and frequency compounding," in *Ultrasonics Symposium, 1996 Proceedings*, 3-6 Nov. 1996, vol. 2, pp. 1097–1101, IEEE.
- [10] R. F. Wagner, M. F. Insana, and S. W. Smith, "Correlation lengths of coherent speckle in medical ultrasonic images," *IEEE Transactions on Ultrasonics, Ferroelectrics, and Frequency Control*, vol. 35, pp. 34–44, Jan. 1988.
- [11] M. O'Donnell and S. D. Silverstein, "Optimum displacement for compound image generation in medical ultrasound," *IEEE Transactions on Ultrasonics, Ferroelectrics, and Frequency Control*, vol. 35, pp. 470–476, July 1988.
- [12] S. W. Smith, R. F. Wagner, J. M. Sandrik, and H. Lopez, "Low contrast detectability and contrast/detail analysis in medical ultrasound," *IEEE Transactions on Sonics and Ultrasonics*, vol. 30, pp. 164–173, May 1983.